Russian Geology and Geophysics © 2019, V.S. Sobolev IGM, Siberian Branch of the RAS
Vol. 60, No. 7, pp. 720–734, 2019 *DOI:10.15372/RGG2019065* *Geologiya i Geofizika*

Bayan-Kol Gabbro–Granite Association (Western Sangilen, Southeastern Tuva): Composition, Age Boundaries, and Tectonic and Geodynamic Settings

I.V. Karmysheva[a,b,] ✉, V.G. Vladimirov[a,b], R.A. Shelepaev[a,b], S.N. Rudnev[a], V.A. Yakovlev[a,b], D.V. Semenova[a]

[a] *V.S. Sobolev Institute of Geology and Mineralogy, Siberian Branch of the Russian Academy of Sciences, pr. Akademika Koptyuga 3, Novosibirsk, 630090, Russia*

[b] *Novosibirsk State University, ul. Pirogova 2, Novosibirsk, 630090, Russia*

Received 13 March 2018; accepted 15 June 2018

Abstract—The Bayan-Kol gabbro–granite association has been recognized within the West Sangilen fragment of collision zone in the northwestern framing of the Tuva–Mongolian massif, and its composition, age, and tectonic and geodynamic settings have been studied. The association includes the Bayan-Kol pluton and composite (mingling) dikes, which formed in the late collision period (495 ± 5 Ma), during the transition from transpression to extension mode with left-lateral strike-slip kinematics. The Bayan-Kol gabbro–granite association is spatially confined to the penetrating tectonic zones of the West Sangilen shear system. The position of gabbroid and granite bodies is controlled by local zones of tectonic extension. Basic magmas have a similar petrogeochemical composition, which indicates their intrusion from a single chamber of basic composition and differentiation of ascending magma. The melting, transfer, and formation of crustal granitoids of the Bayan-Kol association are genetically related to the thermal effect of basic melt and a syntectonic drop in lithostatic pressure. The intrusion and formation of basic and acid melts of the Bayan-Kol association took place at the lower and middle crustal levels in the settings of the reactivation and subsequent fragmentation of the tectonic zone.

Keywords: late-collision magmatism, gabbro–granite associations, collision zone, shear zones, Tuva–Mongolian massif, Sangilen

INTRODUCTION

The existence of a genetic relationship between crustal granitoid melts and basic magmas has been known for a long time and has been widely discussed (Miller and Miller, 2002; Jahn et al., 2009; Jacob et al., 2015). Gabbro–granite series, intrusions, and mingling dikes (composite dikes) are a vivid example of such a relationship (Cook, 1988; Perugini et al., 2005; Sklyarov and Fedorovsky, 2006; Litvinovsky et al., 2017).

A prolonged study of gabbro–granite series of the Altai–Sayan folded area (ASFA)[1] has shown that they can serve as indicators of the mantle–crust interaction in collisional and island-arc geodynamic settings. Of particular significance are gabbro–granite associations of similar ages, i.e., complexes of intrusive rocks of different compositions located in the same tectonic zone and formed in similar tectonic settings in a narrow time interval. Such associations include rocks of different compositions (from basic to acid) but do not always form a single continuous series from gabbroids to granites, with all transitional varieties. Basic and salic rocks in gabbro–granite associations are united by age and structural and tectonic parameters, i.e., their origin, intrusion, and evolution are controlled by a single tectonic regime, but the rocks of contrasting compositions are not genetically related to each other. This is their significant difference from gabbro–granite series forming complexes of plutonic rocks, which are characterized by a close relationship among all rocks, multiphase formation, and homodromous sequence of intrusion (Izokh et al., 1975).

In this work, the possibility of uniting intrusive bodies and the main parameters (tectonic settings, composition, and age) of a single gabbro–granite association are considered by the example of the Bayan-Kol association in the West Sangilen fragment of the ASFA.

GEOLOGIC SETTING

A thorough exploration of western Sangilen has been carried out for several decades (see the review in Kozakov et al., 1999a,b, 2001, 2003; Vladimirov et al., 2005, 2017). In addition to the existing state geological maps of a scale of 1:200,000 (Il'in et al., 1963; Aleksandrov et al., 1974), a number of tectonomagmatic and metamorphic correlations

[1] The research works on this subject are reviewed by Vladimirov et al. (2013).

✉ Corresponding author.
E-mail adress: iri@igm.nsc.ru (I.V. Karmysheva)

and a single geological map of the region have been prepared (Lepezin, 1978; Mitrofanov et al., 1981; Kozakov, 1986; Gonikberg, 1995; Kargopolov, 1997; Kozakov et al., 1999a,b, 2001; Vladimirov et al., 2005, 2017; and other). As a result, a significant amount of data on the geologic structure, magmatism, metamorphism, and isotope-geochronological dating of the region has been accumulated. Many problems, however, remain unresolved, first of all, the subdivision of gabbro–granite intrusive series and their correlation with tectonic and geodynamic settings. The available complex of isotope-geochronological and our structural, petrological, and petrogeochemical data on the chemical composition and tectonic position of magmatic bodies makes it possible to revise the earlier results and make a correlation between magmatic and tectonic events in the region.

Western Sangilen is a fragment of the Cambrian–Ordovician mountain-folded structure resulted from the collision of the Tannu-Ola island arc and the Tuva–Mongolian microcontinent (TMM) (Gibsher et al., 2000; Kuzmichev, 2004; Vladimirov et al., 2005). Three main successive stages of collisional events are recognized in the West Sangilen evolution (Vladimirov et al., 2017): island arc (early collision) (570–535 Ma), collision (535–495 Ma), and late collision (495–430 Ma). The peak of collision events and the beginning of the orogen extension took place at 495 Ma. Each stage is characterized by certain basic and granitoid magmatism. Intrusive processes were most active in the period 510–465 Ma and terminated with the intrusion and development of camptonite dikes of the Agardag alkali-basaltoid complex (442 ± 4 Ma (Gibsher et al., 2012)).

The West Sangilen structure includes the Mugur–Chinchilig (Mugur) and Erzin–Naryn (Nizhnii Erzin) tectonic blocks composed mostly of rocks of the Mugur (Moren) and Nizhnii Erzin metamorphic complexes.

The blocks join each other along the Erzin shear zone (Fig. 1), which is a penetrating area of mylonitization and ductile-plastic flow of rocks (Vladimirov et al., 2005, 2017).

The Erzin zone is formed predominantly by the Erzin metamorphic complex: intensively migmatized cordierite–garnet–biotite gneisses and gneiss-granites. It also includes syntectonic intrusions, e.g., the Matut granite, Bayan-Kol gabbro–granite, and Nizhnii Ulor granite plutons, granitoid bodies of the Ukhadag complex, and abundant composite gabbro–granite dikes (Fig. 1). The main objects of our study were the Bayan-Kol pluton and certain mingling dike bodies.

The Bayan-Kol gabbro–granite pluton is localized in the lower reaches of the Bayan-Kol River, on the right bank of the Erzin River. Two intrusive phases (early and late) are recognized in the gabbroid part of the pluton: I—gabbronorites and II—monzodiorites. The salic part of the pluton includes granodiorites and granites.

Multisystem geochronological data (489 ± 3 Ma, Ar/Ar, Hbl, gabbroids (Isokh et al., 2001); 507 ± 14 Ma, U/Pb, Zrn, granodiorite (Kozakov et al. 2001); and 496.5 ± 3.6 Ma, U/Pb, Zrn, diorite (Kozakov et al., 2001)) suggest that the pluton formed in the period 507 ± 14–497 ± 4 Ma. The younger Ar/Ar date of 489 ± 3 Ma marks the erosion of the Bayan-Kol pluton at the upper levels corresponding to the temperatures of the closure of the K/Ar system in hornblende or reflects repeated thermal events within the Erzin shear zone.

In the west of the Bayan-Kol pluton, granodiorites are hosted by migmatites of the Erzin complex (their chemical composition and the level of metamorphism in the pluton framing are given below). In the north and northeast, gabbroids are hosted by metapelites of the Moren complex, metamorphosed under conditions of moderate- and high-pressure epidote–amphibolite and amphibolite facies (620–700 ºC, 6–8 kbar (Vladimirov, 1987); 550–670 ºC, 7–8 kbar (Kargopolov, 1997)).

Composite (mingling) gabbro–granite dikes in western Sangilen have been known for a long time (Izokh et al., 2004; Vladimirov et al., 2005; Vasyukova et al., 2008; Karmysheva et al., 2015; Burmakina et al., 2016; Vladimirov et al., 2017; Tsygankov et al., 2019). These are products of mechanical mixing and joint consolidation of basic and granitoid magmas of different genesis. In the Erzin tectonic zone they are present as dikes or swarm of dikes and as lenticular or isometric and irregular-shaped bodies. Mingling dikes are hosted by schists and granite-gneisses of the Erzin metamorphic complex and by granites of the Matut pluton.

Mingling dikes in western Sangilen might have formed by different mechanisms of mixing of compositionally contrasting melts (Yakovlev et al., 2016), but all of them are of syntectonic nature (Karmysheva et al., 2015; Vladimirov et al., 2017). One of the main ages of the composite dikes is 495 Ma (Karmysheva et al., 2015; Vladimirov et al., 2017; Tsygankov et al., 2019).

PETROGRAPHY AND CHEMICAL COMPOSITION

Basic rocks

In petrographic composition the gabbroids of the Bayan-Kol pluton correspond to biotite-containing hornblende–olivine and hornblende gabbronorites (phase I) (Opx + CPx + Ol + Pl + Hbl + Bt)[2] and monzodiorites (phase II) (Pl + Cpx + Opx + Hbl + Bt + Kfs ± Qtz). The former have cumulative and poikilitic textures. The cumulus consists of olivine and orthopyroxene, and the intercumulus is composed of clinopyroxene, amphibole, and subordinate plagioclase and biotite. The monzodiorites have an equigranular gabbro-ophitic texture (Shelepaev et al., 2018).

Gabbronorites of phase I are subdivided into melanocratic, mesocratic, and leucocratic (Figs. 2 and 3, Table 1). Melanocratic gabbronorites are rocks of low and normal alkalinity (SiO_2 = 45.37–45.53 wt.% and $Na_2O + K_2O$ = 1.75–

[2] Hereafter, Opx, orthopyroxene; Cpx, clinopyroxene; Ol, olivine; Pl, plagioclase; Hbl, hornblende; Bt, biotite; Prp, pyrope; Qtz, quartz; Sil, sillimanite; Crd, cordierite; Grt, garnet; Alm, almandine; Crs, Cr-spinel; An, anorthite; Ab, albite; Kfs, K-feldspar; Spss, spessartine; Gross, grossular.

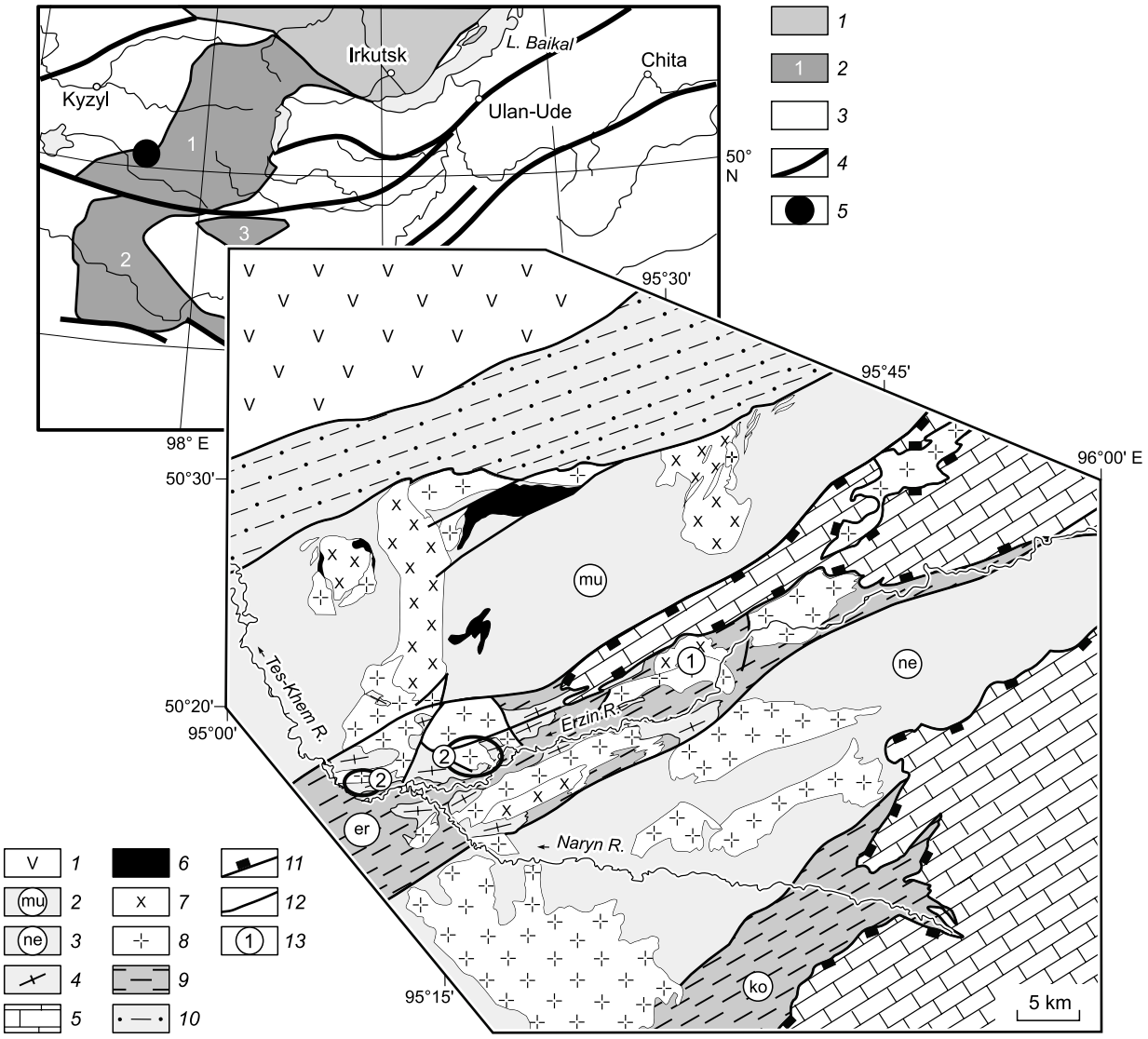

Fig. 1. Schematic geological map of western Sangilen (southeastern Tuva), after Vladimirov et al. (2005) and Karmysheva et al. (2017). Inset shows the position of western Sangilen in the southern framing of the Siberian Platform, after Kuzmichev et al. (2001) and Kuzmichev (2004), simplified. *1*, rocks of the Tannu-Ola island arc; *2–4*, metamorphic complexes: *2*, Mugur, *3*, Nizhnii Erzin, *4*, Erzin; *5*, carbonate-terrigenous cover; *6–8*, igneous rocks: *6*, peridotites, *7*, gabbroids and monzodiorites, *8*, granitoids; *9*, blastomylonites of tectonic zones: Erzin (er), Kokmolgarga (ko); *10*, Agardag suture; *11*, boundaries of nappes; *12*, faults; *13*, objects of study: 1, Bayan-Kol gabbro–granite pluton, 2, areas of mingling dikes. Inset: *1*, Siberian craton; *2*, Precambrian terranes: 1, Tuva–Mongolian massif, 2, Dzavhan massif, 3, Tarbagatai massif); *3*, Paleozoids of the CAOB; *4*, faults; *5*, position of western Sangilen.

2.09 wt.%). Their specific petrochemical feature is high contents of MgO (22.46–24.74 wt.%). Mesocratic varieties contain 10.01–15.07 wt.%. Leucocratic gabbronorites have normal and medium contents of alkalies (SiO_2 = 46.46–52.94 wt.% and $Na_2O + K_2O$ = 2.51–4.72 wt.%), higher contents of TiO_2 (1.15–2.55 wt.%), and MgO = 2.96–8.23 wt.%.

Intrusive phase II is monzodiorites. Their petrochemical characteristics are presented in Table 1 and in Figs. 2 and 3.

The REE patterns of all basic rocks of the pluton have gentle negative slopes; $(La/Yb)_n$ = 5.15–8.48, and $(Eu/Eu^*)_n$ = 0.82–1.67. The multielement patterns show a subduction component, expressed as enrichment of the rocks in LILE (Cs, Rb, U, Th, and K) and Sr and depletion (especially of melanocratic gabbronorites) in HFSE (Ta, Nb, Zr, and Hf) (Fig. 4, Table 2).

Basic rocks of the composite dikes vary widely in composition, from amphibole monzogabbro (Hbl + Kfs + Pl + Bt + Qtz) to diorites (Hbl + Pl + Bt + Qtz). The rocks have a porphyritic texture: Amphibole and biotite form glomerophyric clusters with a cribrate texture. Basites at the contact with the salic component of a dike contain numerous biotite laths, whereas the content of amphibole decreases, up to its disappearance (Karmysheva et al., 2015; Yakovlev et al., 2016; Tsygankov et al., 2019).

Table 1. Contents of major rock-forming components (wt. %) in rocks of the Bayan-Kol pluton and mingling dikes

Component	Bayan-Kol pluton					Mingling dikes	
	Melanocratic gabbronorites	Mesocratic gabbronorites	Leucocratic gabbronorites	Monzodiorites	Granites	Basites	Granites
	$n = 3$	$n = 4$	$n = 9$	$n = 1$	$n = 13$	$n = 13$	$n = 20$
SiO_2	45.37–45.53 / 45.47	46.46–48.56 / 47.22	46.46–52.94 / 49.64	47.49	64.94–74.37 / 69.40	45.48–57.13 / 51.38	61.63–76.37 / 72.49
TiO_2	0.56–0.63 / 0.59	1.13–1.36 / 1.24	1.15–2.55 / 1.88	2.34	0.11–0.87 / 0.54	0.93–1.93 / 1.28	0.07–1.07 / 0.31
Al_2O_3	6.51–7.59 / 6.88	11.54–15.13 / 13.25	15.46–19.88 / 18.32	18.95	14.32–16.61 / 15.19	14.79–17.87 / 16.35	13.20–15.80 / 14.16
Fe_2O_3*	10.46–11.12 / 10.80	9.55–12.35 / 10.89	8.26–13.32 / 10.86	13.07	1.04–5.90 / 4.02	7.49–12.38 / 9.54	1.07–6.02 / 2.39
MnO	0.17–0.18 / 0.17	0.12–0.19 / 0.16	0.12–0.20 / 0.16	0.18	0.02–0.09 / 0.05	0.14–0.17 / 0.15	0.02–0.09 / 0.03
MgO	22.46–24.74 / 23.80	10.01–15.07 / 12.37	2.96–8.23 / 5.18	4.73	0.20–2.44 / 1.26	3.85–9.81 / 6.18	0.19–4.03 / 0.85
CaO	8.61–8.88 / 8.71	6.62–9.69 / 8.64	6.77–10.41 / 8.14	8.04	0.99–4.52 / 2.70	6.08–10.00 / 8.42	0.70–5.29 / 2.06
Na_2O	1.19–1.56 / 1.35	1.96–4.41 / 2.62	2.00–4.01 / 3.23	3.19	2.15–3.58 / 3.06	0.91–4.15 / 3.19	2.65–4.75 / 3.66
K_2O	0.51–0.56 / 0.53	0.35–0.67 / 0.46	0.28–1.48 / 0.72	0.38	1.70–3.67 / 2.66	0.88–2.30 / 1.71	1.17–4.76 / 3.19
P_2O_5	0.09–0.14 / 0.12	1.13–0.47 / 0.27	0.21–0.83 / 0.49	0.89	0.07–0.55 / 0.20	0.27–0.68 / 0.42	0.04–0.40 / 0.12

Note. Above the line, minimum–maximum contents; below the line, average content; *n*, number of analyses.

The mafic component of dikes is formed by rocks of normal and medium alkalinity (Fig. 2, Table 1) (SiO_2 = 45.48–57.13 wt.% and $Na_2O + K_2O$ = 2.82–6.45 wt.%). Most of the rocks have a high content of K_2O (0.88–2.30 wt.%) (Fig. 2). The content of TiO_2 varies from 0.93 to 1.93 wt.%. The REE patterns have a negative slope and show domination of LREE over HREE ($(La/Yb)_n$ = 4.62–8.02) and no Eu anomaly ($(Eu/Eu^*)_n$ = 0.88–1.11). The multielement patterns show enrichment of the rocks in Cs, Rb, U, Th, and K and depletion in Nb, Hf, and Ti (Fig. 4, Table 2).

Salic rocks

Granitoids of the Bayan-Kol pluton are medium-grained biotite granodiorites (Qtz + Pl + Kfs + Bt ± Grt) and medium- to fine-grained granodiorites (Qtz + Pl + Kfs + Bt + Ms) (Karmysheva et al., 2017). These are normal- and medium-alkali (SiO_2 = 64.94–74.37 wt.% and $Na_2O + K_2O$ = 3.85–6.99 wt.%), medium- and high-K (1.70–3.67 wt.%) (Fig. 2, Table 1), predominantly peraluminous (A/CNK = 0.86–1.66) (Fig. 5*a*) granitoids. Their composition varies widely from magnesian to ferroan; most of the rocks are calcareous (Fig. 5*b*, *c*). Their ASI varies from 0.89 to 1.70. Note that only one sample has ASI < 1. In the ASI–SiO_2 diagram, most of the rocks fall in the field of *S*-type granites (Fig. 5*d*). The petrochemical data, the presence of garnet and muscovite among the accessory minerals, and the direct geological observation (see the section "Structural and petrological study") give grounds to assign the salic rocks of the Bayan-Kol pluton to *S*-type granites.

The pluton granitoids have high contents of REE, with domination of LREE over HREE ($(La/Yb)_n$ = 8.37–13.10), and show a negative Eu anomaly (Eu/Eu* = 0.47–0.74) (Fig. 4, Table 2). Their spidergrams show negative Nb, Ti, and Sr anomalies.

The salic component of the mingling dikes varies in composition from granosyenites (Kfs + Pl + Qtz + Bt + Hbl) to leucogranites (Pl + Qtz + Kfs + Bt) (Karmysheva et al., 2015; Yakovlev et al., 2016; Tsygankov et al., 2019). The rocks show wide variations in composition (SiO_2 = 61.63–

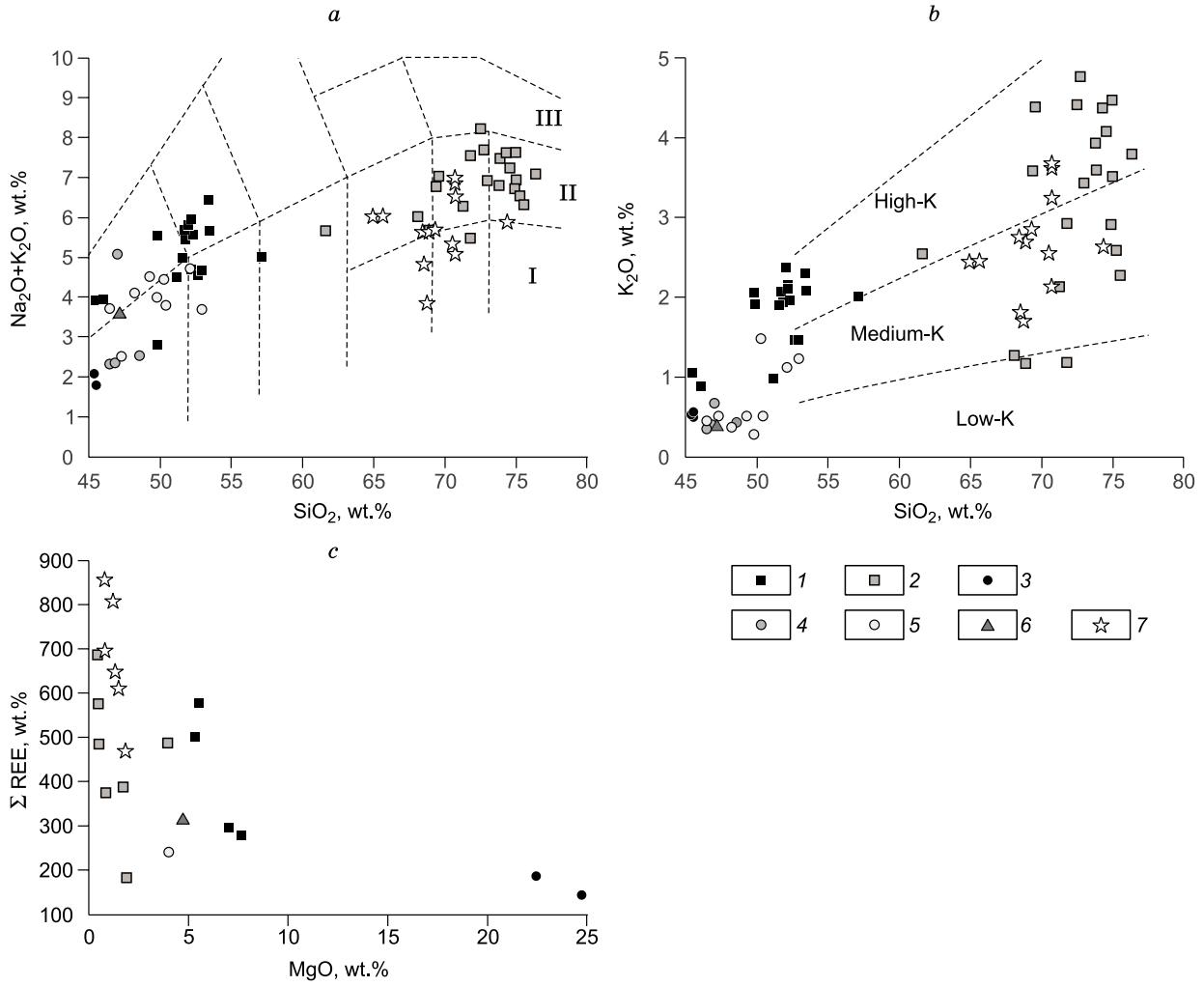

Fig. 2. (Na_2O + K_2O)–SiO_2 (*a*), K_2O–SiO_2 (*b*), and ∑REE–MgO (*c*) diagrams for basites and granitoids of the Bayan-Kol pluton and mingling dikes. *a*, Classification of rocks: I, low-alkali, II, normal-alkali, III, medium-alkali (Petrographic..., 2009); *b*, classification of volcanics, after Le Maitre et al. (1989). *1*, mingling dike basites; *2*, mingling dike granitoids; *3–7*, Bayan-Kol pluton: *3*, melanocratic gabbronorites, *4*, mesocratic gabbronorites, *5*, leucocratic gabbronorites, *6*, monzodiorites, *7*, granitoids.

76.37 wt.% and Na_2O + K_2O = 5.48–8.22 wt.%), being localized mostly in the field of normal-alkali medium-K rocks (Fig. 2, Table 1). In the A/NK–A/CNK diagram they fall predominantly (except for two composition points) in the field of peraluminous varieties (A/CNK = 0.86–1.37) (Fig. 5*a*). They vary in composition from magnesian to ferroan and from calcareous to calc-alkalic rocks (Fig. 5*b*, *c*). Their ASI also varies significantly, from 0.9 to 1.4 (the average is 1.12). By composition, the rocks fall both in the fields of *S*- and *I*-types granites and in the transitional domain (Fig. 5*d*).

The contents of REE vary widely, but all REE patterns have a negative slope and show domination of LREE over HREE ($(La/Yb)_n$ = 4.3–27.26). Salic rocks from different mingling dikes are characterized by both negative and positive Eu anomalies ($(Eu/Eu^*)_n$ = 0.21–1.2). Their multielement patterns show enrichment in Cs, Rb, U, Th, and K and depletion in Nb, Sr, and Ti (Fig. 4, Table 2).

STRUCTURAL AND PETROLOGICAL STUDY

The Bayan-Kol gabbro–granite pluton. At the northeastern contact of the Bayan-Kol pluton, where gabbroids intruded metapelites of the Mugur complex, the host rocks show subvertical deformations. In the vertical sections of exposures, biotite–sillimanite–cordierite schists have plastic cordierite–biotite interbeds with extension structures and drag folds composed of quartz–plagioclase material (Fig. 6*a*, *b*).

In the contact aureole of gabbroids of the Bayan-Kol pluton, there is a wide range of mineral phases reflecting both regional and contact metamorphism related to the intrusion of basic melts. Contact metamorphism minerals are quartz, plagioclase, cordierite, garnet, sillimanite, and biotite. Garnets form clusters with synkinematic-rotation and dissolution structures. The pressure shadows around them are formed by cordierite, biotite, and quartz (Fig. 6*d*). Sillimanite is confined to *C*/*S*-type stretching structures (Fig. 6*c*).

Table 2. Contents of major components (wt.%) and trace and rare-earth elements (ppm) in representative samples of rocks of the Bayan-Kol pluton

Component	Granites						Melanocratic gabbronorites		Leucocratic gabbronorite	Monzodiorite	Salic component							Diorites		Gabbro	
	AG-327	AG-316	AG-315	AG-324	P-667	AG-332/1	Sh3-00	Sh107-15	I18-99	Sh109-15	Y-68-3	Y-68-4	Y-68-8A	Y-68-8B	Y-68-10	KT-1002-2	Y-69-10	Y-69-12	Y-69-7	7-153-1	7-153-2
SiO_2	68.53	70.74	70.53	69.32	70.70	65.65	45.52	45.53	48.21	47.49	76.37	74.97	69.38	69.57	61.63	74.56	71.79	49.82	52.32	45.48	46.05
TiO_2	0.70	0.45	0.56	0.66	0.56	0.72	0.56	0.63	2.01	2.34	0.21	0.25	0.60	0.68	1.07	0.21	0.36	1.47	1.31	1.64	1.93
Al_2O_3	14.88	15.07	14.88	15.07	14.68	16.19	6.51	7.59	19.46	18.95	13.20	13.55	14.11	13.67	15.16	13.68	14.86	17.87	17.07	15.40	15.68
FeO*	4.91	3.27	4.26	4.54	3.57	5.03	10.46	11.12	11.77	13.07	1.93	2.20	4.92	5.32	6.02	2.01	3.30	10.43	9.45	12.17	12.38
MnO	0.06	0.03	0.02	0.06	0.06	0.06	0.17	0.17	0.20	0.18	0.03	0.03	0.06	0.07	0.09	0.03	0.03	0.17	0.15	0.15	0.16
MgO	1.50	0.81	1.22	1.33	0.80	1.84	24.74	22.46	4.02	4.73	0.48	0.44	1.73	1.90	4.03	0.51	0.86	5.51	5.33	7.66	7.05
CaO	2.68	2.26	2.40	2.40	2.22	3.25	8.64	8.61	8.14	8.04	0.84	0.70	1.81	1.39	5.29	1.05	3.31	8.16	7.53	9.36	10.00
Na_2O	3.02	3.28	2.79	2.84	3.23	3.58	1.29	1.19	3.74	3.19	3.30	3.16	3.19	2.65	3.13	3.16	4.30	3.50	3.60	2.87	3.06
K_2O	1.81	3.24	2.55	2.85	3.62	2.45	0.51	0.56	0.37	0.38	3.79	4.47	3.58	4.38	2.54	4.08	1.18	2.05	1.96	1.05	0.88
P_2O_5	0.15	0.18	0.18	0.19	0.15	0.25	0.12	0.14	0.55	0.89	0.05	0.06	0.05	0.05	0.40	0.16	0.17	0.61	0.48	0.27	0.27
LOI	0.91			0.85	0.90	1.00	1.06	1.04	1.19	0.49	0.69	0.87	0.81	0.69	0.72	1.26	0.85	1.39	0.99	1.81	1.84
Total	99.15	99.33	99.39	100.11	100.49	100.02	99.58	99.43	99.66	99.54	100.33	99.98	99.59	99.86	99.51	99.63	100.24	99.74	99.35	97.86	99.29
Th	13.5	15.0	17.9	14.6	17.6	8.2	1.07	1.31	0.63	0.65	21	33	7.5	3.3	11.4	19.4	10.6	2.8	3.2	1.08	1.17
U	1.06	1.00	1.06	1.00	1.23	1.15	0.37	0.42	0.16	0.27	2.8	2.4	0.94	0.59	4.0	3.2	1.81	3.0	3.9	0.36	0.33
Rb	92	80	114	96	106	113	8.83	9.95	4.79	4.27	81	91	106	118	76	84	27	45	49	19.05	11.65
Ba	1 067	1 360	1 472	1 170	1 211	800	132.9	186.84	138.44	159.97	772	999	779	1 072	629	1 155	377	554	577	173.18	181.16
Sr	252	248	333	259	245	327	238.2	335.83	540.20	801.30	147	155	191	178	438	212	568	616	623	438.73	459.42
La	44	53	58	46	60	33	7.25	10.24	15.08	17.96	37	46	30	17.4	28	30	33	32	31	13.30	13.78
Ce	85	102	115	89	117	65	15.34	22.14	29.70	38.35	70	90	59	31	57	66	68	74	64	29.00	30.66
Pr	10.1	12.5	13.6	10.8	14.4	7.7	2.14	3.03	3.72	5.31	8.4	10.8	7.0	3.4	8.1	7.1	6.3	10.4	9.1	4.25	4.51
Nd	39	47	51	42	55	29	10.28	12.71	16.20	23.37	30	39	26	12.1	33	26	21	42	36	17.89	19.51
Sm	8.8	10.3	11.7	8.9	12.3	6.6	2.22	2.72	3.37	4.50	6.5	7.8	4.4	1.67	6.5	5.3	3.9	8.7	7.2	4.16	4.45
Eu	1.75	1.68	2.2	1.49	1.87	1.62	0.63	0.72	1.75	1.70	0.60	0.57	0.74	0.64	1.32	0.68	0.67	2.6	2.0	1.59	1.67
Gd	8.0	8.9	11.0	9.0	11.7	6.7	1.99	2.61	2.93	4.37	6.8	8.4	4.3	1.57	6.6	5.6	3.2	7.4	6.6	4.53	4.88
Tb	1.02	1.10	1.47	1.17	1.51	0.94	0.34	0.45	0.41	0.62	1.21	1.32	0.62	0.19	1.05	0.94	0.46	1.10	0.91	0.67	0.73
Dy	5.4	5.1	7.6	6.3	8.1	4.6	1.86	2.39	2.28	3.39	8.2	8.8	3.4	0.85	6.0	6.6	2.7	6.0	5.4	3.86	4.09
Ho	1.16	1.05	1.48	1.35	1.69	0.87	0.39	0.45	0.49	0.62	1.78	1.96	0.62	0.15	1.25	1.38	0.51	1.21	0.95	0.78	0.81
Er	3.2	2.8	4.1	3.6	5.0	2.5	1.06	1.34	1.22	1.72	5.5	5.8	1.73	0.43	3.6	4.3	1.59	3.3	2.8	2.13	2.20
Tm	0.50	0.42	0.60	0.57	0.76	0.34	0.20	0.19	0.18	0.23	0.91	0.92	0.28	0.070	0.57	0.68	0.26	0.46	0.40	0.30	0.32
Yb	3.3	2.7	3.8	3.5	4.9	2.3	0.95	1.13	1.26	1.43	5.7	5.6	1.82	0.43	3.7	4.7	1.70	3.0	2.6	1.94	1.99
Lu	0.46	0.39	0.50	0.48	0.66	0.32	0.14	0.16	0.16	0.21	0.86	0.88	0.28	0.065	0.57	0.70	0.26	0.45	0.39	0.28	0.30
Zr	317	260	354	280	315	218	37.54	55.43	8.69	48.49	137	170	237	247	184	135	175	183	169	133.48	142.17
Hf	7.8	6.4	8.8	7.0	7.9	5.4	0.94	1.27	0.28	1.05	4.6	5.6	6.4	6.4	5.3	4.3	5.2	4.2	3.9	3.33	3.46
Ta	0.69	0.49	0.73	0.69	0.63	0.65	0.03	0.18	0.30	0.51	0.81	0.75	0.67	0.54	1.80	1.77	1.05	0.59	0.51	0.78	0.78
Nb	10.7	9.1	12.3	10.4	9.7	9.7	1.01	3.72	10.81	8.99	7.9	9.9	11.9	10.0	30	13.2	7.8	11.0	9.1	13.30	12.84
Y	42	34	53	45	58	34	11.28	14.31	13.13	19.32	55	60	18.5	4.6	38	42	16.1	33	29	23.91	25.50
$(La/Yb)_n$	8.89	13.10	10.46	8.74	8.37	9.76	5.15	6.09	8.07	8.48	4.30	5.52	11.19	27.26	4.95	4.32	12.92	7.22	8.02	4.62	4.67
Eu/Eu*	0.62	0.53	0.59	0.50	0.47	0.74	0.90	0.82	1.67	1.16	0.27	0.21	0.51	1.20	0.61	0.38	0.56	0.98	0.88	1.11	1.09

Table 3. Representative compositions of biotite in biotite–sillimanite–cordierite schists of the contact aureole of the Bayan-Kol pluton gabbroids

Component	M-343		
	1	2	3
SiO_2, wt.%	35.02	35.17	35.46
TiO_2	2.49	2.01	1.84
Al_2O_3	19.34	20.03	19.43
FeO	18.49	18.76	18.68
MgO	9.64	9.69	10.45
MnO	0.03	0.02	0.04
Na_2O	0.15	0.13	0.15
K_2O	8.38	7.85	8.26
Total	93.65	93.76	93.46
Si, apfu	2.69	2.68	2.71
Ti	0.14	0.12	0.11
Al	1.75	1.80	1.75
Fe^{2+}	1.19	1.20	1.13
Mg	1.10	1.10	1.19
Mn	0	0	0
Na	0.02	0.02	0.02
K	0.82	0.76	0.81
Fe/(Fe + Mg)	0.52	0.52	0.49

Note. Here and in Tables 4–6, minerals were analyzed with a Camebax-Micro electron probe (analyst O.S. Khmel'nikova, Institute of Geology and Mineralogy, Novosibirsk).

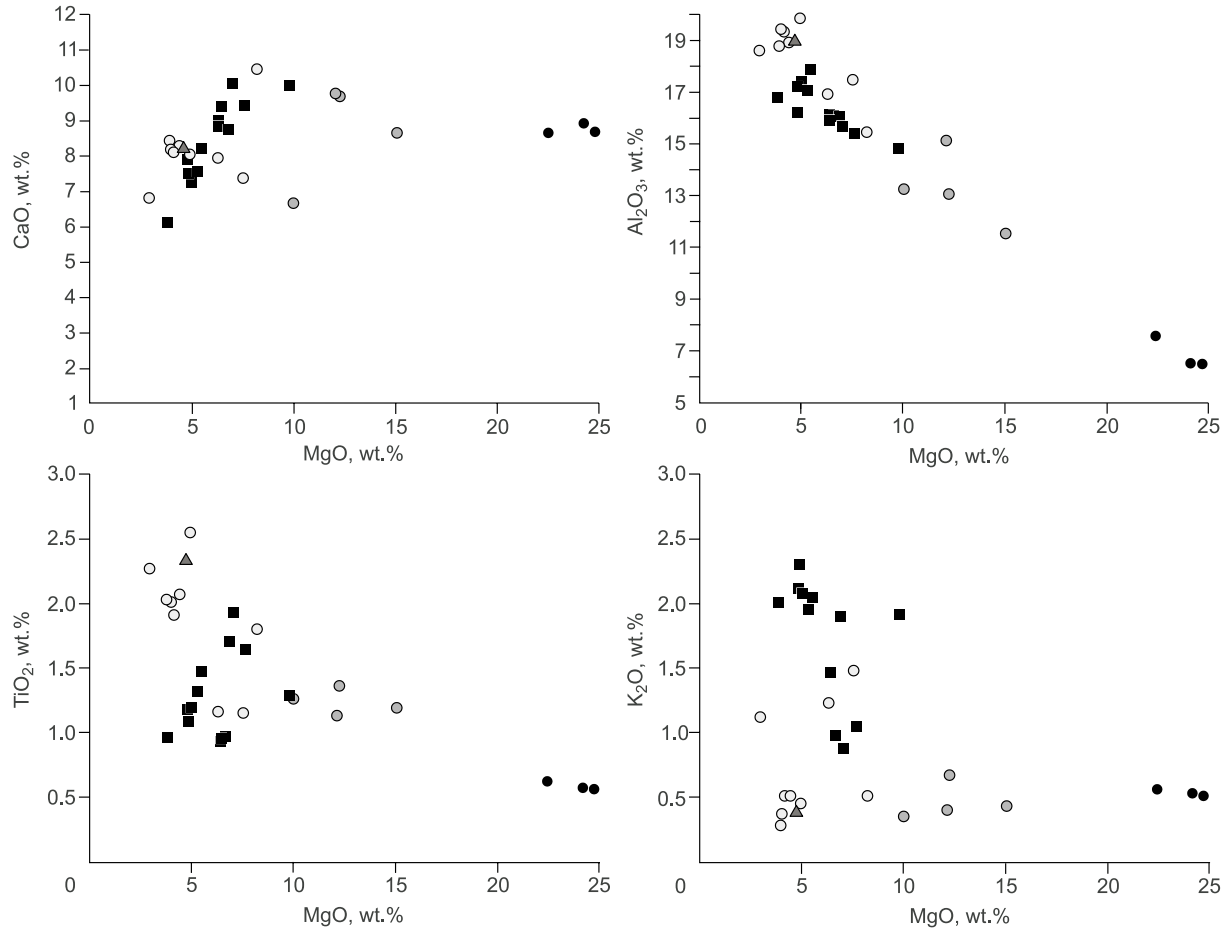

Fig. 3. CaO–MgO, Al_2O_3–MgO, TiO_2–MgO, and K_2O–MgO diagrams for basites of the Bayan-Kol pluton and mingling dikes. Designations follow Fig. 2.

Table 4. Representative compositions of garnet in biotite–sillimanite–cordierite schists of the contact aureole of the Bayan-Kol pluton gabbroids

Component	M-343						
	1	2	3	4	5	6	7
SiO_2, wt.%	37.24	36.80	36.85	36.63	36.64	37.08	36.89
Al_2O_3	21.11	20.77	21.00	20.63	20.72	20.86	20.85
FeO	35.26	36.52	35.83	36.49	36.12	34.75	35.08
MgO	3.91	3.32	3.89	3.23	3.42	4.33	4.24
MnO	1.35	1.25	1.14	1.29	1.24	1.25	1.47
CaO	0.77	0.63	0.61	0.95	0.83	0.75	0.58
Na_2O	0.02	0.04	0.01	0.03	0.04	0.02	0.02
Total	99.74	77.50	99.47	99.36	99.07	99.14	99.32
Si, apfu	3.00	2.99	2.98	2.98	2.99	3.00	2.98
Al	2.00	1.99	2.00	1.98	1.99	1.99	1.99
Fe^{2+}	2.38	2.48	2.43	2.49	2.46	2.35	2.37
Mg	0.47	0.40	0.47	0.39	0.42	0.52	0.51
Mn	0.09	0.09	0.08	0.09	0.09	0.09	0.10
Na	0	0.01	0	0.01	0.01	0	0
Ca	0.07	0.06	0.05	0.08	0.07	0.07	0.05
X_{Alm}	0.79	0.82	0.80	0.82	0.81	0.78	0.78
X_{Prp}	0.16	0.13	0.15	0.13	0.14	0.17	0.17
X_{Spss}	0.03	0.03	0.03	0.03	0.03	0.03	0.03
X_{Gross}	0.02	0.02	0.02	0.03	0.02	0.02	0.02
Fe/(Fe + Mg)	0.83	0.86	0.84	0.86	0.86	0.82	0.82

Table 5. Representative compositions of cordierite in biotite–sillimanite–cordierite schists of the contact aureole of the Bayan-Kol pluton gabbroids

Component	M-343					
	1	2	3	4	5	6
SiO_2, wt.%	48.58	49.00	47.82	48.54	48.11	48.00
Al_2O_3	32.96	32.95	32.50	32.80	32.62	32.96
FeO	7.77	7.44	7.92	7.89	7.85	7.79
MgO	8.66	8.65	8.68	8.52	8.75	8.74
MnO	0.07	0.09	0.06	0.07	0.05	0.07
Na_2O	0.13	0.21	0.10	0.08	0.10	0.17
Total	98.22	98.48	97.14	97.94	97.54	97.76
Si, apfu	5.00	5.02	4.98	5.01	4.99	4.96
Al	3.99	3.98	3.99	3.99	3.98	4.02
Fe^{2+}	0.67	0.64	0.69	0.68	0.68	0.67
Mg	1.33	1.32	1.35	1.31	1.35	1.35
Mn	0.01	0.01	0.01	0.01	0.01	0.01
Na	0.03	0.04	0.02	0.02	0.02	0.03
Fe/(Fe + Mg)	0.33	0.33	0.34	0.34	0.33	0.33

According to kinematics and the direction of mineral lineation, the deformations in oriented petrographic thin sections are normal-reverse faults.

Biotite often occurs unconformably with the general elongate mineral lineation of rocks. Its postkinematic structure seems to be related to postdeformational static recrystallization at the regressive stage during the rapid cooling of rocks. This is also indicated by the low content of TiO_2 (1.84–2.49, Table 3) in the mineral (Ushakova, 1971).

The pressures and temperatures in the aureole of gabbroids at the northeastern contact of the Bayan-Kol pluton were calculated based on the synkinematic parageneses Qtz + Pl_{25} + Grt_{85} + Crd_{33} + Sil (Tables 4–6): 600–620 ºC and 4.3 kbar (Fig. 7).

At the western contact of the Bayan-Kol polyphase pluton, granitoids are in contact with migmatites of the Erzin complex. At the exocontact, granites alternate with migmatites, and in the endocontact zone, there are numerous shad-

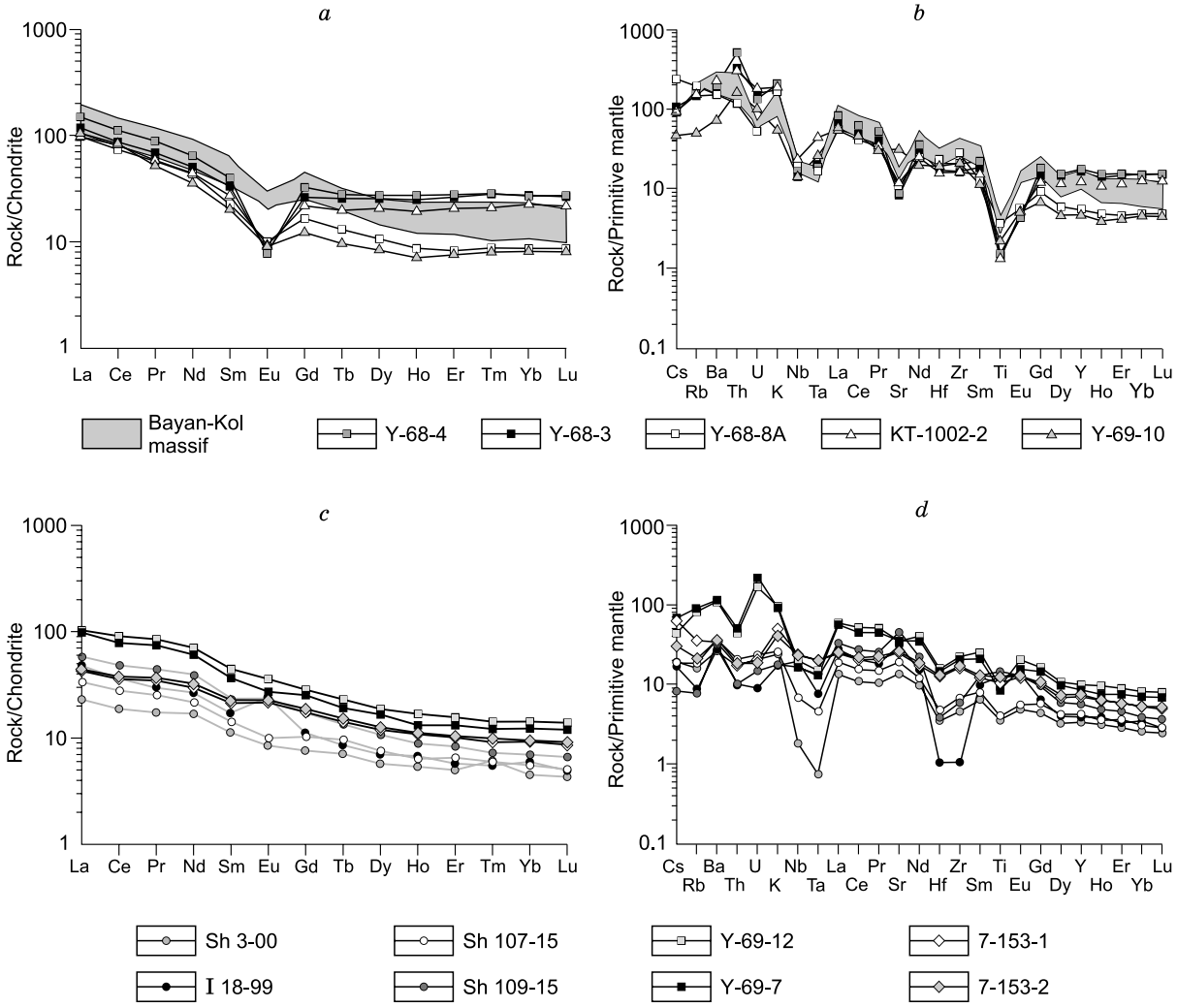

Fig. 4. Chondrite CI-normalized (Boynton, 1984) REE patterns and primitive-mantle-normalized (Taylor and McLennan, 1985) spidergrams of basites and granitoids of the Bayan-Kol pluton and mingling dikes. *a–b,* Granites; *c–g*, basites.

ow structures of the host metamorphic rocks (Fig. 6*e*). The migmatites bear signs of melting and segregation of the produced granite melt (Fig. 6*f*). The *P–T* conditions of metamorphism and granite formation are estimated at 790 ºC and 5.4 kbar. Sinistral ductile-plastic deformations are superposed on migmatite–granites of the Erzin complex (Karmysheva et al., 2017).

Mingling dikes show plastic, brittle–plastic, and brittle deformations. Gabbroids are characterized by ductile-plastic fragmentation with passive filling of the cavities with acid melts, by drag and flow structures, and by elements of reverse-fault structures, namely, indicator *C*/*C′*-type structures formed by granite veinlets (Fig. 8).

There are often brittle deformations inside dikes, such as fracturing of basite fragments, with fractures filled with acid melt generated from the host granitoids. Sometimes, the structures resemble “magmatic breccias” formed by breaking of basic nodules, with cavities filled with a pegmatoid material.

Table 6. Representative compositions of plagioclase in biotite–sillimanite–cordierite schists of the contact aureole of the Bayan-Kol pluton gabbroids

Component	M-343		
	1	2	3
SiO_2, wt.%	61.80	63.05	61.08
Al_2O_3	23.89	23.45	24.49
Na_2O	8.83	8.99	8.32
CaO	5.38	4.87	5.92
Total	100.05	100.50	99.93
Si, apfu	2.74	2.78	2.72
Al	1.25	1.22	1.28
Na	0.76	0.77	0.72
Ca	0.26	0.23	0.28
X_{An}	0.25	0.23	0.28
X_{Ab}	0.75	0.77	0.72

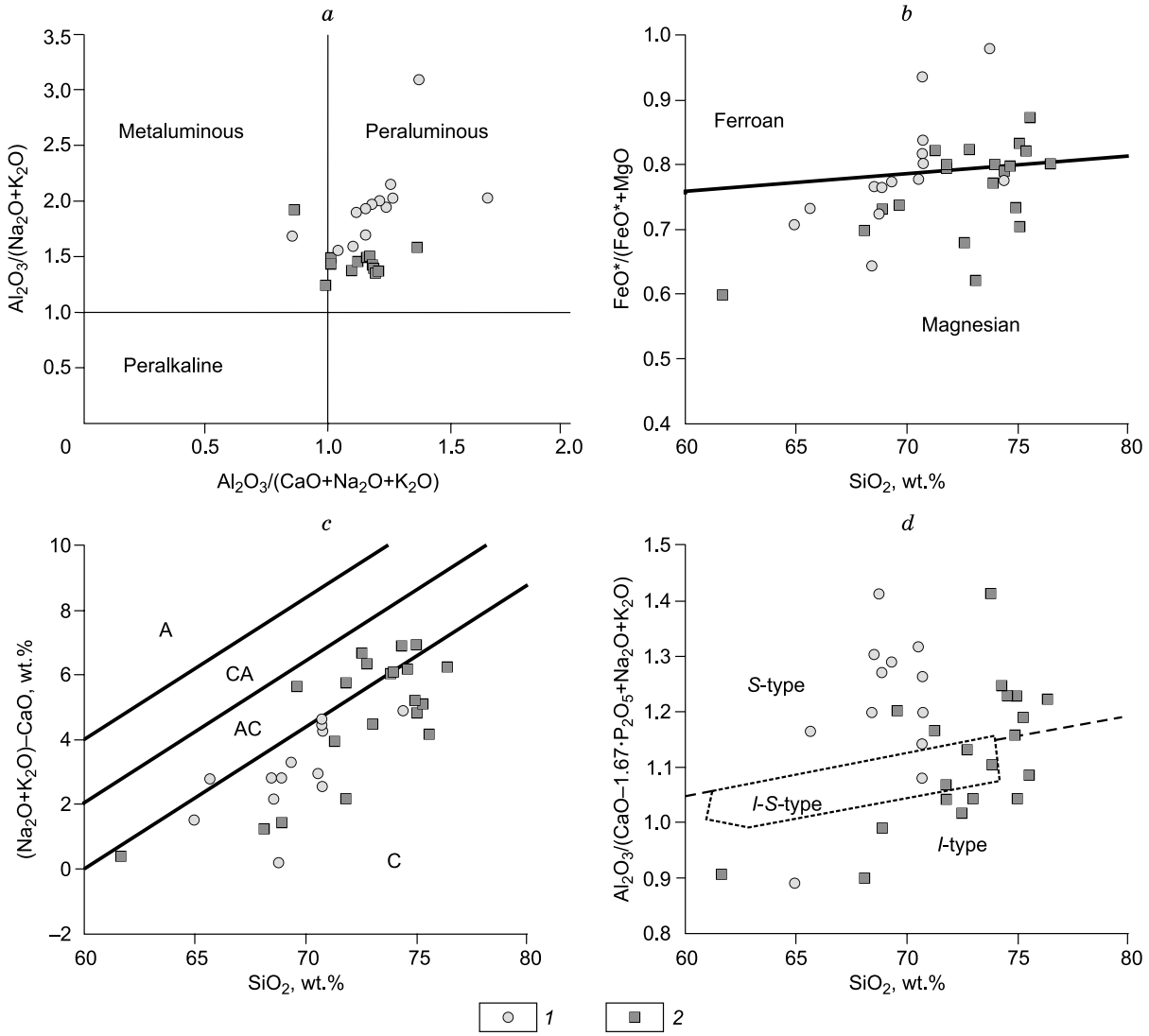

Fig. 5. $Al_2O_3/(Na_2O + K_2O)$–$Al_2O_3/(CaO + Na_2O + K_2O)$ (Maniar and Piccoli, 1989) (*a*), FeO*/(FeO* + MgO)–SiO_2 (Frost et al., 2001) (*b*), $(Na_2O + K_2O – CaO)$–SiO_2 (Frost et al., 2001) (*c*), and $Al_2O_3/(CaO – 1.67P_2O_5 + Na_2O + K_2O)$–$SiO_2$ (Liew et al., 1989) (*d*) diagrams for rocks: C, calcareous; AC, alkali-calcareous; CA, calc-alkalic; A, alkaline; *1,* granitoids of the Bayan-Kol pluton; *2*, granitoids of mingling dikes.

The rocks of the basic component of dikes have extension structures with mineral linearity conformable with biotite. At the contact with the salic component of dikes, there are sometimes prismatic aggregates of hornblende and plagioclase linearly stretching along the contact.

DISCUSSION

The stage of 495 ± 5 Ma in the West Sangilen evolution is marked by the peak of collision events and a change of the transression regime to the transtension one (Vladimirov et al., 2017). Compression with shear led to a decrease in the total lithostatic pressure, fragmentation, and reactivation of the Erzin tectonic zone, followed by the formation of local pull-apart zones within it. These settings favored the ascent of basic melts to the lower and middle crustal levels, which led to an additional heating of the host rocks.

The pressures and temperatures of the contact aureole of the Bayan-Kol pluton gabbroids (600–620 ºC and 4.3 kbar) confirm the intrusion of the pluton into a low-pressure zone. Comprehensive structural study of the contact aureole (syn-kinematic growth of contact metamorphism mineral phases and indicative kinematic structures in the host rocks) unambiguously shows a vertical motion of basic melt and involvement of the contact rocks in deformations. The change in the rheological behavior of the host rocks and their hornfelsing suggest that the intrusion of basic magmas served as an additional source of heat for the host metapelites and for the anatectic melting-out of granites and granodiorites and that the shear deformations led to the separation and motion of the acid melt.

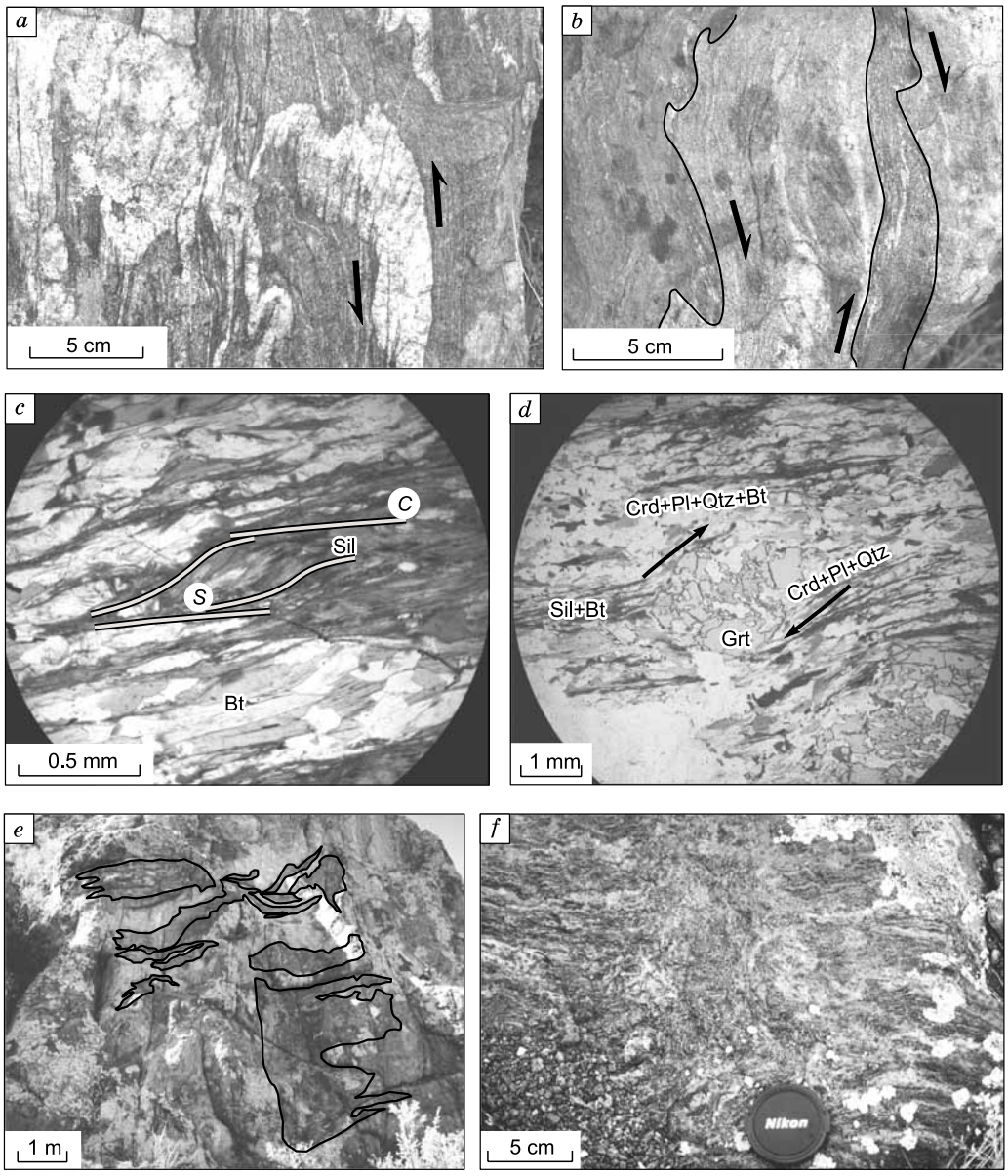

Fig. 6. Indicators of syntectonic intrusion of gabbroids (*a–d*) and granite formation in the Bayan-Kol gabbro–granite massif (*e*, *f*). *a, b*, Plastic-flow and drag folds in the host biotite–sillimanite–cordierite schists (northeastern contact); *c*, indicative *C*/*S*-type extension structures composed of sillimanite (aureole of gabbroids at the northeastern contact); *d*, rotation and dissolution of garnet, accompanied by the growth of newly formed mineral phases (cordierite, quartz, and plagioclase) in low-pressure zones (aureole of gabbroids at the northeastern contact); *e*, shadow migmatite structures in granodiorites (southwestern contact); *f*, segregation of granite melt in migmatites of the Erzin complex (southwestern contact of granites).

The isotope-geochronological investigations showed that some mingling dikes in the Erzin tectonic zone also formed at 495 Ma. Our structural and petrological studies demonstrated that the intrusion and formation of the Bayan-Kol pluton and the described composite dikes took place in the same tectonic settings. As in the Bayan-Kol pluton, basites intruded along pull-apart fractures in local low-pressure zones. Additional heating from basic melts and drop in lithostatic pressure led to the melting of the host rocks and the formation of new portions of granite melt, which filled pull-apart fractures in the partly crystallized basites. Melts of contrasting compositions in West Sangilen mingling dikes mixed by different mechanisms (Yakovlev et al., 2016; Vladimirov et al., 2017; Tsygankov et al., 2019), but all the mechanisms included the intrusion of basites into low-pressure zones with tectonic deformations (Table 7).

The petrochemical data show a difference in the compositions of the basic component of mingling dikes and of basic rocks of the Bayan-Kol pluton. In contrast to gabbroids of the Bayan-Kol pluton, basites of mingling dikes have

Table 7. Characteristics of the Bayan-Kol gabbro–granite association

Parameter	Bayan-Kol polyphase gabbro–granite pluton	Composite (mingling) gabbro–granite dikes
Geodynamic position	Collisional mountain-folded structure of Cambrian–Ordovician age formed under collision of the Tannu-Ola island arc and the Tuva–Mongolian microcontinent	
Geodynamic settings	Postcollisional period in the evolution of the collision zone, characterized by the transition from transpression to transtension with left-lateral strike-slip kinematics	
Tectonic position	In the Erzin tectonic zone, in areas of local extension	
Tectonic settings	Reactivation of the Erzin tectonic zone at 495 Ma, followed by sinistral subhorizontal deformations and fragmentation of this zone	
Isotope-geochronological data (basites)	489 ± 3 Ma, Ar/Ar, Hbl (Izokh et al., 2001); 496.5 ± 3.6 Ma, U/Pb, Zrn (Kozakov et al., 1999)	484.7 ± 12 Ma, U/Pb, Zrn; 490 ± 16 Ma, U/Pb, Zrn (Tsygankov et al., 2019)
Isotope-geochronological data (granites)	507 ± 14 Ma, U/Pb, Zrn (Kozakov et al., 2001)	494.9 ± 4.5 Ma, U/Pb, Zrn; 479.1 ± 24 Ma, U/Pb, Zrn (Tsygankov et al., 2019)
Basic rocks		
Petrographic composition	Biotite-containing hornblende–olivine and hornblende gabbronorites (Opx + Cpx + Ol + Pl + Hbl + Bt), monzodiorites (Pl + Cpx + Opx + Hbl + Bt + Kfs ± Qtz)	Amphibole monzogabbro (Hbl + Kfs + Pl + Bt + Qtz), diorites (Hbl + Pl + Bt + Qtz)
Contents of major components, wt.%	SiO_2 = 45.37–52.94 $Na_2O + K_2O$ = 1.75–5.08 TiO_2 = 0.56–2.55 MgO = 2.96–24.74 (see also Table 1)	SiO_2 = 45.48–57.13 $Na_2O + K_2O$ = 2.82–6.45 TiO_2 = 0.93–1.93 MgO = 3.85–9.81 (see also Table 1)
Petrogeochemical features	$(La/Yb)_n$ = 5.15–8.07 $(Eu/Eu^*)_n$ = 0.9–1.67 enriched in Cs, Rb, U, Th, K, and Sr and depleted in Ta, Nb, Zr, and Hf	$(La/Yb)_n$ = 4.62–8.02 $(Eu/Eu^*)_n$ = 0.88–1.11 enriched in Cs, Rb, U, Th, and K and depleted in Nb, Hf, and Ti
Salic rocks		
Petrographic composition	Biotite granodiorites (Qtz + Pl + Kfs + Bt + Grt + Hbl), granites (Qtz + Pl + Kfs + Bt + Ms)	Granosyenites (Qtz + Pl + Kfs + Bt + Hbl), leucogranites (Qtz + Pl + Kfs + Bt)
Contents of major components, wt.%	SiO_2 = 64.94–74.37 $Na_2O + K_2O$ = 3.85–6.99 K_2O = 0.70–3.67 A/CNK = 0.86–1.66	SiO_2 = 61.63–76.37 $Na_2O + K_2O$ = 5.48–8.22 K_2O = 1.17–4.76 A/CNK = 0.86–1.37
Petrogeochemical features	$(La/Yb)_n$ = 8.37–13.10 $(Eu/Eu^*)_n$ = 0.47–0.74 depleted in Nb, Ti, and Sr	$(La/Yb)_n$ = 4.3–27.26 $(Eu/Eu^*)_n$ = 0.21–1.2 depleted in Nb, Ti, and Sr

MgO < 11 wt.%. Magnesian compositions are typical of the melanocratic Bayan-Kol gabbroids with crypt and cumulative textures, which indicates the accumulation of olivine. In general, the compositions of the Bayan-Kol basites reflect the differentiation of basic melt inside a magma chamber (Shelepaev et al., 2018). More differentiated leucocratic gabbronorites are most similar in the contents of MgO, CaO, and TiO_2 to the basic component of mingling dikes. Leucocratic gabbronorites of the Bayan-Kol pluton are richer in alumina (15.46–19.88 wt.%) but are somewhat poorer in K_2O (0.28–1.48 wt.%) than the basites of mingling dikes (14.79–17.87 and 0.88–2.30 wt.%, respectively). The different composition of the mingling dike basites might be due to the interaction of basic and acid magmas and the enrichment of the basites with crustal material.

The average contents of trace and rare-earth elements in the basic component of mingling dikes are higher than those in gabbroids of the Bayan-Kol pluton. The REE content in these basites is even higher than the REE content in some salic rocks of the mingling dikes (Fig. 2*c*). The increase in the content of HREE cannot be explained by the impact of acid melt, but it might be due to an increase in the content of incompatible elements during the fractionation of the parental basic magma in intermediate chambers. The intrusion of residual melts enriched in incompatible elements and forming the basic component of mingling dikes is confirmed by their petrochemical correlation with differentiated leucocratic gabbronorites and monzodiorites of the Bayan-Kol pluton.

The salic material of dikes shows a wide variation in composition ($Na_2O + K_2O$ = 5.48–8.22 wt.%, A/CNK =

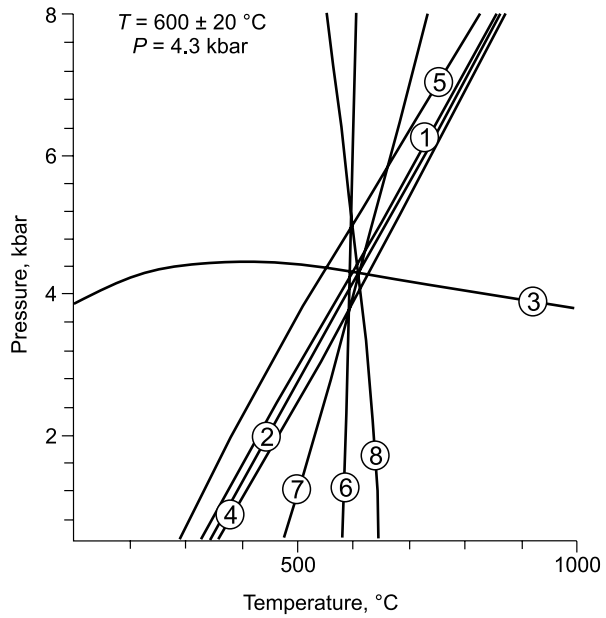

Fig. 7. Parameters of metamorphism in the contact aureole of the Bayan-Kol pluton gabbroids. Temperatures and pressures were calculated using the TWQ 2.02 software (Berman and Aranovich, 1996). 1, 4Sil + 5*b*Qtz + 2Alm = 3*f*Crd; 2, 2Sil + *b*Qtz + Grs = 3An; 3, 4Sil + 5*b*Qtz + 2Prp = 3Crd; 4, 6Sil + 5Grs + 3*f*Crd = 2Alm + 15An; 5, 2Alm + 6An + 3bQtz = 2Grs + 3*f*Crd; 6, 3Crd + 2Alm = 3*f*Crd + 2Prp; 7, 3Crd + 5Grs + 6Sil = 2Prp + 15An; 8, 6An + 2Prp + 3*b*Qtz = 2Grs + 3Crd.

0.86–1.37) because of its different sources. In one case, the salic component formed at the expense of a fine-grained granite dike cut by basites, which led to the formation of mingling structures (Yakovlev et al., 2016). In other cases, the compositions of the salic magmatic components of composite dikes are determined by the host rocks, namely, biotite–garnet granites of the Erzin complex and porphyraceous (Kfs) biotite–amphibole granites of the Matut pluton. The partial melting and rheomorphism of these rocks resulted in an acid melt, which filled viscous extension fractures in basites of composite dikes.

Despite the wide variations in composition, the salic rocks of the Bayan-Kol pluton and mingling dikes do not differ seriously in major petrogeochemical parameters. The origin and transition of granite material were caused by a drop in pressure under change in tectonic regime and by the additional heating during the intrusion of basic melt along weakened zones.

CONCLUSIONS

The recognition of the Bayan-Kol gabbro–granite association in western Sangilen was based on the results of our structural and petrological studies, which give an insight into the regime and mechanisms of intrusion of melts of different compositions in a limited period of syncollisional tectonic activity. The available isotope-geochronological data made it possible to determine the time interval of the formation of the studied objects. The petrogeochemical data confirmed that gabbroids of the Bayan-Kol pluton and coeval mingling dikes have much in common. The performed research permitted us to unite these rocks into an association and recognize its key characteristics:

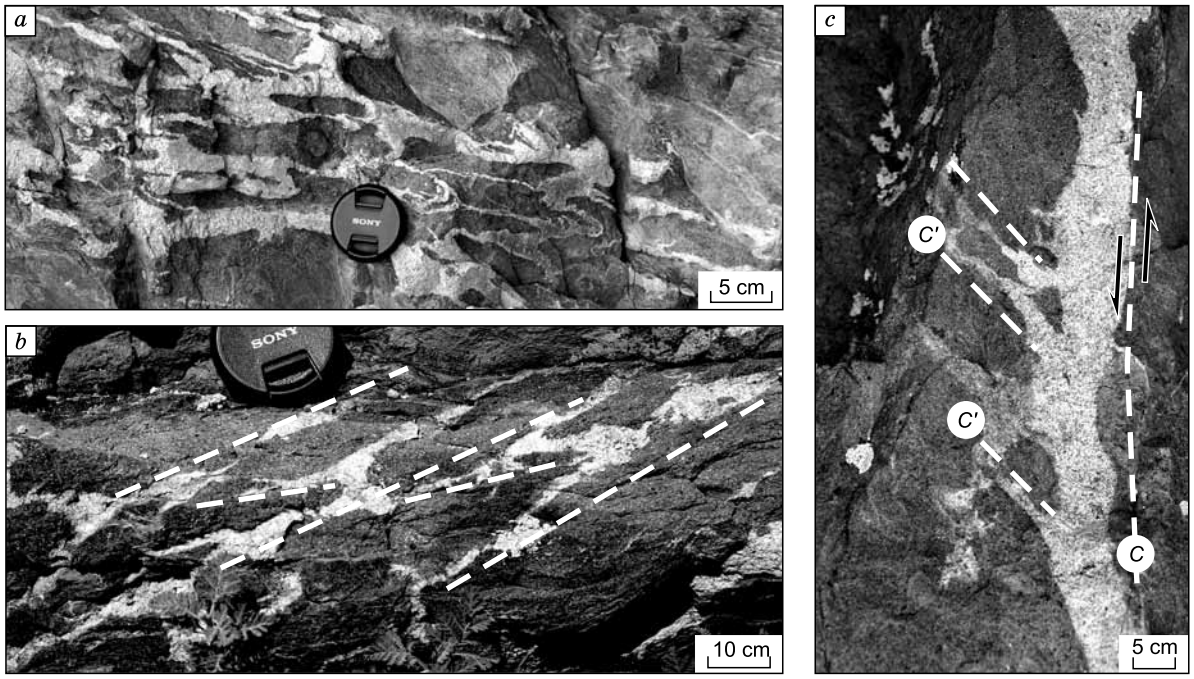

Fig. 8. Magmatic mingling structures. *a*, Ductile-plastic flow and extension of basic nodules and granite melt; *b*, filling of basite extension fractures with granite material; *c*, subvertical *C*/*C′* extension structures formed by mingling dike granites.

(1) Intrusion and evolution of mantle basic and crustal granitoid magmas took place at 495 ± 5 Ma, at the beginning of the late collision stage of evolution of the West Sangilen fragment of collisional orogen on the northwestern margin of the Tuva–Mongolian microcontinent.

(2) Gabbro–granite associations are confined to penetrating tectonic zones of the West Sangilen shear system. The position of gabbroid and granite bodies is controlled by local zones of tectonic extension.

(3) The basic magmas are similar in petrogeochemical composition, which indicates their intrusion from the same chamber of basic composition and differentiation of ascending magma.

(4) The melting, transition, and evolution of crustal granitoids of the Bayan-Kol association are genetically related to the thermal effect of basic melt and the syntectonic drop in lithostatic pressure.

(5) The Bayan-Kol gabbro–granite association should be assigned to the collisional syntectonic type forming in the lower–middle crust.

The work is done on state assignment of IGM SB RAS. The study was financially supported by grants 16-05-01011, 18-05-00851, 18-05-00105, 18-35-00467, and 18-35-00484 from the Russian Foundation for Basic Research and project 5.1688.2017/PCh of the Ministry of Education and Science of the Russian Federation.

REFERENCES

Aleksandrov, G.P., Zhuravleva, Z.A., Stepanova, M.V., 1974. Stratigraphy of Early Proterozoic Sangilen deposits, in: Materials on the Geology of the Tuvinian ASSR [in Russian]. Kyzyl, Issue 3, pp. 3–22.

Berman, R.G., Aranovich, L.Y., 1996. Optimized standard state and solution properties of minerals: I. Model calibration for olivine, orthopyroxene, cordierite, garnet, and ilmenite in the system FeO–MgO–CaO–Al_2O_3–TiO_2–SiO_2. Contr. Miner. Petrol. 126, 1–24.

Boynton, W.V., 1984. Cosmochemistry of the rare earth elements; meteorite studies, in: Henderson, P. (Ed.), Rare Earth Element Geochemistry. Elsevier, Amsterdam, pp. 63–114.

Burmakina, G.N., Tsygankov, A.A., Khubanov, V.B., Vladimirov, V.G., Karmysheva, I.V., Buyantuev, M.D., 2016. Composite dikes in western Sangilen, southeastern Tuva: isotopic age, composition, and petrogenesis, in: Correlation between Altaides and Uralides: Magmatism, Metamorphism, Stratigraphy, Geochronology, Geodynamics, and Metallogeny. Proceedings of the Third International Scientific Conference, Novosibirsk, 29 March–1 April 2016 [in Russian]. IGM SO RAN, Novosibirsk, pp. 35–37.

Cook, N.D.J., 1988. Diorites and associated rocks in the Anglem Complex at the Neck, northeastern Stewart Island, New Zealand: an example of magma mingling. Lithos 21, 247–262.

Frost, B.R., Barnes, C.G., Collins, W.J., Arculus, R.J., Ellis, D.J., Frost, C.D., 2001. A geochemical classification for granitic rocks. J. Petrol. 42 (3), 2035–2048.

Gibsher, A.A., Vladimirov, A.G., Vladimirov, V.G., 2000. Geodynamics of the Early Paleozoic thrust-and-fold structure of the Sangilen, southeastern Tuva. Dokl. Earth Sci. 370 (1), 50–53.

Gibsher, A.A., Malkovets, V.G., Travin, A.V., Belousova, E.A., Sharygin, V.V., Konc, Z., 2012. The age of camptonite dikes of the Agardag alkali-basalt complex (western Sangilen): results of Ar/Ar and U/Pb dating. Russian Geology and Geophysics (Geologiya i Geofizika) 53 (8), 763–775 (998–1013).

Gonikberg, V.E., 1995. Geologic Structure and Tectonic Nature of the Early Caledonian Margin of the Sangilen Massif in Tuva. PhD Thesis [in Russian]. Moscow.

Il'in, A.V., Moralev, V.M., 1963. Precambrian strata in the Altai–Sayan area. Sovetskaya Geologiya, No. 21, 51–58.

Izokh, A.E., Kargopolov, S.A., Shelepaev, R.A., Travin, A.V., Egorova, V.V., 2001. Cambrian–Ordovician basic magmatism in the Altai–Sayan folded area and related high-temperature low-pressure metamorphism, in: Topical Issues of Geology and Minerageny of Southern Siberia. Proceedings of Scientific and Practical Conference, Elan' Village, Kemerovo Region, 31 October–2 November 2001 [in Russian]. Novosibirsk, pp. 68–72.

Izokh, A.E., Lavrenchuk, A.V., Vasyukova, E.A., 2004. Dike complex in western Sangilen, manifestation of Ordovician mantle magmatism, in: Geodynamic Evolution of the Lithosphere of the Central Asian Mobile Belt (from Ocean to Continent). Proceedings of Scientific Meeting on the Basic Research Program [in Russian]. Institut Geografii SO RAN, Irkutsk, Vol. 1, pp. 143–144.

Izokh, E.P., Yudalevich, Z.A., Ponomareva, A.P., Sukhin, M.V., Mushkin, I.V., Shmulevich, G.D., Pyatkov, K.K., Pyanovskaya, I.A., Sandomirskii, G.G., 1975. Formational Analysis of Granitoids in Western Uzbekistan [in Russian]. Nauka, Novosibirsk.

Jacob, K.H., Farmer, G.L., Buchwaldt, R., Bowring, S.A., 2015. Deep crustal anatexis, magma mixing, and the generation of epizonal plutons in the Southern Rocky Mountains, Colorado. Contrib. Mineral. Petrol. 169 (1), Article 7.

Jahn, B.M., Litvinovsky, B.A., Zanvilevich, A.N., Reichow, M., 2009. Peralkaline granitoid magmatism in the Mongolian–Transbaikalian Belt: Evolution, petrogenesis and tectonic significance. Lithos 113, 521–539.

Kargopolov, S.A., 1997. HT-LP Granulites in Western Sangilen (Southeastern Tuva). PhD Thesis [in Russian]. IG SO RAN, Novosibirsk.

Karmysheva, I.V., Vladimirov, V.G., Vladimirov, A.G., Shelepaev, R.A., Yakovlev, V.A., Vasyukova, E.A., 2015. Tectonic position of mingling dikes in the accretion–collisional system of early Caledonides in western Sangilen (southeastern Tuva). Geodyn. Tectonophys. 6 (3), 289–310.

Karmysheva, I.V., Vladimirov, V.G., Vladimirov, A.G., 2017. Synkinematic granitoid magmatism of western Sangilen, south-east Tuva. Petrology 25 (1), 87–113.

Kozakov, I.K., 1986. Precambrian Infrastructural Complexes in Mongolia [in Russian]. Nauka, Leningrad.

Kozakov, I.K., Kotov, A.B., Sal'nikova, E.B., Bibikova, E.V., Kovach, V.P., Kirnozova, T.I., Berezhnaya, N.G., Lykhin, D.A., 1999a. The age of metamorphism of crystalline complexes of the Tuva–Mongolian massif: results of U–Pb geochronological studies of granitoids. Petrologiya 7 (2), 174–190.

Kozakov, I.K., Sal'nikova, E.B., Bibikova, E.V., Kirnozova, T.I., Kotov, A.B., Kovach, V.P., 1999b. The polychronous evolution of Paleozoic granitoid magmatism in the Tuva–Mongolian massif: results of U–Pb dating. Petrologiya 7 (6), 631–643.

Kozakov, I.K., Kotov, A.B., Salnikova, E.B., Kovach, V.P., Natman, A., Bibikova, E.V., Kirnozova, T.I., Todt, W., Kröner, A., Yakovleva, S.Z., Lebedev, V.I., Sugorakova, A.M., 2001. Timing of the structural evolution of metamorphic rocks in the Tuva–Mongolian massif. Geotectonics 35 (3), 165–184.

Kozakov, I.K., Kovach, V.P., Yarmolyuk, V.V., Kotov, A.B., Sal'nikova, E.B., Zagornaya, N.Yu., 2003. Crust-forming processes in the geologic development of the Tuva–Mongolia massif: Sm–Nd isotopic and geochemical data for granitoids. Petrology 11 (5), 444–463.

Kuzmichev, A.B., 2004. Tectonic History of the Tuva–Mongolian Massif: Early Baikalian, Late Baikalian, and Early Caledonian Stages [in Russian]. PROBEL-2000, Moscow.

Kuzmichev, A.B., Bibikova, E.V., Zhuravlev, D.Z., 2001. Neoproterozoic (similar to 800 Ma) orogeny in the Tuva–Mongolia Massif (Siberia): island arc-continent collision at the northeast Rodinia margin. Precambrian Res. 110 (1–4), 109–126.

Le Maitre, R.W., Bateman, P., Dudek A., Keller, J., Lameyre Le Bas, M.J., Sabine, P.A., Schmid, R., Sorensen, H., Streckeisen, A., Woolley, A.R., Zanettin, B., 1989. A Classification of Igneous Rocks and a Glossary of Terms. Blackwell Scientific Publications, Oxford.

Lepezin, G.G., 1978. Metamorphic Complexes in the Altai–Sayan Folded Area [in Russian]. Nauka, Novosibirsk.

Liew, T.C., Finger, F., Höck, V., 1989. The Moldanubian granitoid plutons of Austria: chemical and isotopic studies bearing on their environmental setting. Chem. Geol. 76, 41–55.

Litvinovsky, B.A., Zanvilevich, A.N., Wickham, S.M., Jahn, B.M., Vapnik, Y., Kanakin, S.V., Karmanov, N.S., 2017. Composite dikes in four successive granitoid suites from Transbaikalia, Russia: The effect of silicic and mafic magma interaction on the chemical features of granitoids. J. Asian Earth Sci. 136, 16–39.

Maniar, P.D., Piccoli, P.M., 1989. Tectonic discrimination of granitoids. Geol. Soc. Am. Bull. 101, 635–643.

Miller, C.F., Miller, J.S., 2002. Contrasting stratified plutons exposed in tilt blocks, Eldorado Mountains, Colorado River Rift, NV, USA. Lithos 61, 209–224.

Mitrofanov, F.P., Kozakov, I.K., Palei, I.P., 1981. The Precambrian in Western Mongolia and Southern Tuva [in Russian]. Nauka, Leningrad.

Perugini, D., Poli, G., Rocchi, S., 2005. Development of viscous fingering between mafic and felsic magmas: evidence from the Terra Nova Intrusive Complex (Antarctica). Mineral. Petrol. 83, 151–166.

Petrographic Code of Russia. Igneous, Metamorphic, Metasomatic, and Impact Rocks [in Russian], 2009. Izd. VSEGEI, St. Petersburg.

Shelepaev, R.A., Egorova, V.V., Izokh, A.E., Zeltman, R., 2018. Collisional mafic magmatism of the fold–thrust belts framing southern Siberia (Western Sangilen, southeastern Tuva). Russian Geology and Geophysics (Geologiya i Geofizika) 59 (5), 525–540 (653–672).

Sklyarov, E.V., Fedorovsky, V.S., 2006. Magma mingling: tectonic and geodynamic implications. Geotectonics 40 (2), 120–134.

Taylor, S.R., McLennan, S.M., 1985. The Continental Crust: Its Evolution and Composition. Blackwell, London.

Tsygankov, A.A., Burmakina, G.N., Yakovlev, V.A., Khubanov, V.B., Vladimirov, V.G., Karmysheva, I.V., Buyantuev, M.D., 2019. Composition and U–Pb (LA–ICP-MS) isotopic age of zircons from composite dikes of western Sangilen (Tuva–Mongolian orogen). Russian Geology and Geophysics (Geologiya i Geofizika) 60 (1), 45–66 (55–78).

Ushakova, E.N., 1971. Biotites of Metamorphic Rocks [in Russian]. Nauka, Moscow.

Vasyukova, E.A., Izokh, A.E., Lavrenchuk, A.V., 2008. Petrology of Ordovician syngranite dikes (western Sangilen, southeastern Tuva), in: Geodynamic Evolution of the Lithosphere of the Central Asian Mobile Belt (from Ocean to Continent). Proceedings of Scientific Meeting on Integration Programs of the Department of Geosciences, Siberian Branch of the Russian Academy of Sciences [in Russian]. IZK SO RAN, Irkutsk, Vol. 1, pp. 56–58.

Vladimirov, A.G., Izokh, A.E., Polyakov, G.V., Babin, G.A., Mekhonoshin, A.S., Kruk, N.N., Khlestov, V.V., Khromykh, S.V., Travin, A.V., Yudin, D.S., Shelepaev, R.A., Karmysheva, I.V., Mikheev, E.I., 2013. Gabbro–granite intrusive series and their indicator importance for geodynamic reconstructions. Petrology 21 (2), 158–180.

Vladimirov, V.G., 1987. Near-contact deformations of metamorphites of the Mugur Formation in the area of the Moren and Solcher Rivers (southwestern Sangilen), in: Integrated Geological Exploration of Sangilen (Southeastern Tuva). Collection of Research Papers [in Russian]. IGiG SO AN SSSR, Novosibirsk, pp. 67–88.

Vladimirov, V.G., Vladimirov, A.G., Gibsher, A.S., Travin, A.V., Rudnev, S.N., Shemelina, I.V., Barabash, N.V., Savinykh, Ya.V., 2005. Model of the tectonometamorphic evolution for the Sangilen block (southeastern Tuva, Central Asia) as a reflection of the Early Caledonian accretion–collision tectogenesis. Dokl. Earth Sci. 405 (8), 1159–1165.

Vladimirov, V.G., Karmysheva, I.V., Yakovlev, V.A., Travin, A.V., Tsygankov, A.A., Burmakina, G.N., 2017. Thermochronology of mingling dikes in western Sangilen (southeastern Tuva): evidence for a breakdown of a collisional system on the northwestern margin of the Tuva–Mongolian massif. Geodyn. Tectonophys. 8 (2), 283–310.

Yakovlev, V.A., Karmysheva, I.V., Vladimirov, V.G., 2016. Geologic and structural characteristics of mingling dikes of the Erzin tectonic zone (western Sangilen, southeastern Tuva), in: Petrology of Igneous and Metamorphic Rock Associations. Issue 8. Proceedings of the Russian Petrographic Conference with International Participation [in Russian]. Izd. Tomskogo TsNTI, Tomsk, pp. 365–370.

Editorial responsibility: N.N. Kruk